Article:
Barco, A, Ingham, E orcid.org/0000-0002-9757-3045, Fisher, J orcid.org/0000-0003-3833-3700 et al. (2 more authors) (2018) On the design and efficacy assessment of self-assembling peptide-based hydrogel-glycosaminoglycan mixtures for potential repair of early stage cartilage degeneration. Journal of Peptide Science, 24 (8-9). e3114. ISSN 1075-2617

https://doi.org/10.1002/psc.3114

On the design and efficacy assessment of self-assembling peptide-based hydrogel-glycosaminoglycan mixtures for potential repair of early stage cartilage degeneration.

A.Barco,[a] E. Ingham,[a] J. Fisher,[a] H. Fermor,[a] and R.P.W. Davies [b]

a. Institute of Medical and Biological Engineering, Leeds, United Kingdom.
b. Department of Oral Biology, Leeds, United Kingdom.

Peptide-based hydrogels are of interest for their potential use in regenerative medicine. Combining these hydrogels with materials that may enhance their physical and biological properties, such as glycosaminoglycans (GAGs), has the potential to extend their range of biomedical applications, for example in the repair of early cartilage degeneration. The aim of this study was to combine three self-assembling peptides (SAPs) (P_{11}-4, P_{11}-8 and P_{11}-12) with chondroitin sulphate at two molar ratios of 1:16 and 1:64 in 130 mM and 230 mM Na^+ salt concentrations. The study investigates the effects of mixing SAP and GAG on the physical and mechanical properties at 37ºC. Peptide alone, chondroitin sulphate alone and peptide in combination with chondroitin sulphate were analysed using Fourier transform infrared (FTIR) spectroscopy to determine the β-sheet percentage, transmission electron microscopy (TEM) to determine the fibril morphology and rheology to determine the elastic and viscous modulus of the materials. All of the variables (peptide, salt concentration and chondroitin sulphate molar ratio) had an effect on the mechanical properties, β-sheet formation and fibril morphology of the hydrogels. P_{11}-4 and P_{11}-8-chondroitin sulphate mixtures, at both molar ratios, were shown to have a high β-sheet percentage, dense entangled fibrilar networks as well as high mechanical stiffness in both (130 mM and 230 mM) Na^+ salt solutions when compared to the P_{11}-12/chondroitin sulphate mixtures. These peptide/ chondroitin sulphate hydrogels show promise for biomedical applications in glycosaminoglycan depleted tissues.

Introduction

The poor regenerative capacity of human articular cartilage contributes to the development of debilitating osteoarthritis (OA) and remains a major clinical challenge. Osteoarthritis is a disease which contributes to 2.8% disability adjusted life years amongst high income countries.(1) Around nine million people in the UK have sought treatment for OA and of these, 4.71 million are related to knee OA, which could increase to 8.3 million by 2035.(2) A net depletion of glycosaminoglycan's (GAGs) in osteoarthritic cartilage has been reported in the literature.(3, 4) This has been shown to result in the loss of mechanical properties and function in vitro, and is considered to be a major contributor to disease progression.(5)

There is considerable interest in the development of novel early interventions to repair or replace damaged cartilage. Delaying the progression of severe OA will subsequently reduce the need for joint replacement. One approach to repair early cartilage degradation is to restore GAG levels with the aim of maintaining functional cartilage material properties.(5, 6)

Peptides are of a particular interest and have been shown to readily self-assemble into higher order structures that create very stable hydrogels under physiological conditions. They have been used to develop novel materials for regenerative medicine applications.(7-19) The P_{11}-X family of self-assembling peptides(SAPs) are rationally designed to form a hierarchy of supramolecular structures which include single molecule thick tapes, ribbons (double tapes), fibrils (stacks of ribbons) and fibres (entangled fibrils). The design principles include an odd number of amino acids which

maximises intermolecular interactions driving anti-parallel beta-sheet formation. They are based on polar amino acids, which form strong intermolecular interactions (polar zippers) increasing β-tape stability. They have alternating polar/apolar side chains situated in the middle of the peptide, maximising β-strand formation. Hydrophobic residues (trp, phe) are placed in the middle of the peptide and on the same side in order to drive ribbon formation. Finally, charged residues were included to drive anti-parallel β-sheet formation and impart 'a trigger' to induce hierarchical assembly by virtue of the protonation and deprotonation of the charged moieties. The P_{11}-X family and their physico-chemical properties have been studied extensively.[6, 14, 20, 21] The SAPs in this study, have the ability to form hydrogels form an initial non Newtonian fluid state upon application of a trigger, they have been shown to be biocompatible and studies have indicated that they have potential as a visco-supplementation treatment for early stage OA.[8, 14]. P_{11}-4 is a glutamine-based peptide with a net negative charge at physiological pH, Similarly P_{11}-8 is also glutamine based but it has a net positive charge at physiological pH. For P_{11}-12 the glutamine residues are replaced with serine residues, this will have the effect of increasing the relative hydrophilicity whilst maintaining the same charge distribution and pH phase behaviour P_{11}-8. The combination of SAPs with GAGs may provide increased bio-functionality and additionally they have the ability to be delivered in a minimally invasive manner. This makes them ideal candidates for use as injectable materials and potential effective interventions for early stage OA.

A key challenge is the control over the mechanical properties of these hydrogels which can be affected by the concentration of the peptide, the net charge of the peptide and also the environmental conditions such as pH and ionic strength.[20, 22] For potential application in the treatment of early stage OA, SAP-GAG mixtures with three favourable properties would be desirable: High β-sheet percentage (which is pivotal, as the hierarchical supramolecular structures formed are dependent on the amount of β-sheet formed), long-woven fibrilar networks and a high stiffness. All of which must occur in specific physiological conditions.

Previous studies have shown that the addition of large amounts of GAG does not inhibit self-assembly of P_{11}-4, 8 and 12 when in a physiological buffer of phosphate buffered solution (PBS).[22] We are exploring the efficacy of this SAP/GAG multicomponant system in conditions specifically realted to cartilage. Imperitive to fulfil its function as an anchor in the cartilage for delivering GAGs, our SAP/GAG system would be required to be a stable gel over time. Our system should not show any shear thining at fequencies including (but not limited to) that of walking frequency, which is ca. 1Hz (60 strides per minute).[24]
Rheology is used to mimic the mechanical process that these hydrogels may undergo, such as the shear of cartilage under load. Walking frequency (stride length) is ca. 1Hz (60 strides per minute).[24, 25] Therefore, the rheological behaviour of the assembled peptides and assembled SAP/GAG mixtures were compared at this frequency.

The overall aim of this work is to develop a system whereby GAGs are delivered into the surface of GAG depleted cartilage using a carrier self-assembling peptide. The SAPs would initially be delivered as a non-viscous fluid. Subsequently once in place the SAPs are triggered by the natural environment to self-assemble (into hierarchical supramolecular structures-driven by β-sheet formation) and induce anchorage of applied GAG. In this study, we therefore; 1) Determine the β-sheet percentage in model physiological conditions; 2) Assess the fibril morphology and 3) Determine the biomechanical properties (stiffness) of three SAPs, P_{11}-4, P_{11}-8 and P_{11}-12 (Table 1). The effects of combining the SAPs with chondroitin sulphate (GAG) at two molar ratios of 1:16 and 1:64 in 130 mM and 230 mM Na^+ salt solutions, which are

representative of normal physiological conditions and the physiological environment within the surface of articular cartilage were considered.

Table 1

Results and discussion

Cartilage contains varying counter ions, the amounts and species depend on the region of the cartilage and are important to its biomechanical function.[23] Urban summarised the range of ion concentration in two discreet areas of the cartilage, at the surface ($[Na^+]$ 210-230 mM, $[K^+]$ 7mM $[Ca^{2+}]$ 4-6 mM, $[Cl^-]$ 100-110 mM) and in deep cartilage ($[Na^+]$ 260-320 mM, $[K^+]$ 9-11 mM, $[Ca^{2+}]$ 8-15 mM, $[Cl^-]$ 70-90 mM). Our focus is in replacing GAG depletion near the surface and fixing it in place with a hydrogel network. It is important to investigate the behaviour of SAPs and SAP-GAG mixtures in the relevant physiological conditions.

Secondary structure- Fourier transform infrared (FTIR)

The β-sheet formation of the SAPs is central to the proposed mechanism of action in replacing depleted GAGs in cartilage. FTIR analysis was used to study the secondary structure of peptides; P_{11}-4, P_{11}-8 and P_{11}-12 in the presence and absence of chondroitin sulphate at molar ratios of 1:16 and 1:64 in two concentrations of Na^+ salt solution. The primary structure of the de-novo SAPs studied are designed so that they adopt a β-sheet conformation, which can be identified in the amide I region using FTIR.[26-28]

The FTIR data shows that the self-assembled peptide conformation is rich in β-sheet for all three SAPs (alone) in both Na^+ salt solutions and in most of the SAP-GAG mixtures in both Na^+ salt solutions, as demonstrated in Figure 1. Of particular interest, was the relative β-sheet percentage formed by the SAPs alone, which are indicative of self-assembled hydrogel state.[29, 30] Increasing the Na^+ ion concentration had different effects depending on the SAP. SAP P_{11}-4 at the higher Na^+ salt concentration indicated a slight decrease in the percentage of β-sheet formed, which is possibly due to the monovalent cation interaction in the unassembled (monomeric) state. The monovalent cations could interact with the negatively charged peptide forming an electric layer around the negatively charged monomer, which in turn increases the energy barrier for β-sheet formation, preventing self-assembly. For P_{11}-8 and P_{11}-12 the percentage of β-sheet formed increased (Figure 1), as these monomeric peptides carry a net positive charge, there is a repulsion of cations and no increase in the energy barrier for β-sheet formation. This shows the potential effects of the surrounding environment on the biochemical properties of the peptide.

Figure 1

The addition of chondroitin sulphate at molar ratios of 1:16 and 1:64 in conjunction with the two varying concentrations of Na^+ ions in the salt solutions had a very different effect on the percentage of β-sheet formed. A small addition of GAG to P_{11}-4 (1:64) caused the peaks observed in the region of 1672-1690cm^{-1} (anti-parallel β-sheet conformation) to decrease in intensity. This indicated a decrease in the percentage of β-sheet formed compared to the peptide alone (Figure 1). Interestingly, the addition of more GAG (1:16) caused an increase in the overall percentage β-sheet. This could indicate that a small addition of GAG disrupted the ability of the peptide to self-assemble due to the electrostatic repulsion between the highly negatively charged

GAG molecules and the negatively charged peptide, while the addition of more GAG seemed to drive the self-assembly further (Figure 1). A similar effect was seen when comparing P_{11}-4 at the same GAG molar ratio and increasing the concentration of Na^+ ions in the salt solution. This could be explained by the screening of electrostatic repulsions between the positive and negative side chains of P_{11}-4 with the increasing concentration of Na^+ ions.

Conversely, the addition of a small amount of GAG to P_{11}-8 and P_{11}-12 in the 130 mM Na^+ salt solution caused the percentage of β-sheet formed to initially increase but as more GAG was added the percentage of β-sheet formed decreased, more so in P_{11}-12 than P_{11}-8 (Figure 1). Nevertheless, it is important to note that the use of GAG with P_{11}-12 had a detrimental effect on the percentage of β-sheet formed, specifically at the higher GAG molar ratio (Figure 1).

As with all techniques, FTIR has its limitations especially when used to analyse peptidic hydrogels [31], as these biomaterials are very sensitive to the way they are treated. The biphasic solutions/gels analysed in the FTIR can dissociate upon the application of mechanical force between the CaF_2 discs, resulting in sheer thinning. This leads to a disproportionate amount of gel and fluid between the IR discs which could lead to inaccurate determination of β-sheet content. However, every effort was made to reduce this with the use of a known path length of 0.025mm. Nevertheless due to the concentration regime and aqueous salt conditions used, FTIR was the only available means in assessing the conformation of the system studied. Despite the possible limitations of the technique FTIR analysis clearly highlighted that two of the three SAPs (P_{11}-4 and P_{11}-8) demonstrated a greater percentage of β-sheet in the presence of the GAG at 130mM and 230mM Na^+ salt concentrations, when compared to P_{11}-12. This higher percentage of β-sheet, demonstrates that self-assembly has taken place at physiological conditions and makes P_{11}-4 and P_{11}-8, good candidates to take forward into biological studies, depending on their fibril morphology and biomechanical properties. The formation of peptide gels are subject to a difference in the kinetics of self-assembly which can be influenced by the surrounding conditions and the molar ratio of GAG. Therefore, the values of β-sheet percentage presented in this study may not be indicative of values that the peptide and peptide-GAG mixtures may have achieved if they had been left to reach a full equilibrium state. The SAP/GAG multicomponent systems were investigated two days after initial preparation, to replicate the practical application.

Hydrogel morphology and fibril formation - TEM

Physical differences between the fibre morphology of the different samples were observed by TEM. Representative images are shown in Figure 2, Figure 3 and Figure 4. Varying networks of entangled fibres or bundles were observed, which are essential for gel formation. Overlapping of the fibrils and fibres made it difficult to definitively assess the morphology, hence regions in which individual fibrils could clearly be observed were chosen to measure the lengths and widths. The peptides in different salt solutions exhibited a twist pitch, meaning two widths were recorded; a wide width and a narrow width (where the twist occurred), values of width and twist pitch are presented in Figure 5. Average lengths ranging from ca. 410 to 990 nm for the peptides alone and ca. 498 to 3518 nm for the peptide-GAG mixtures were recorded (Figure 6).

Figure 2

Figure 3

Figure 4

The effect that the Na^+ ion concentration in the salt solution and the GAG molar ratio had on the lengths and widths of the fibrils formed varied from peptide to peptide. For P_{11}-4 and P_{11}-8, Na^+ ion concentration in the salt solution, GAG molar ratio and their combined effects all had a significant effect (2-way ANOVA; $p<0.05$) on the morphology of the fibrils. The data indicates that in the 230 mM Na^+ salt solution, the P_{11}-4 fibrils were longer than in the 130 mM Na^+ salt solution.
Interestingly, for P_{11}-8 there were multiple types of structure observed. Fibrils were by far the most frequent structure but there were instances of nanotube formation. P_{11}-8 fibrils were longer in the 130 mM Na^+ salt solution when compared to the P_{11}-8 fibrils in the 230 mM Na^+ salt solution. For P_{11}-12, only the GAG molar ratio had a significant effect (2-way ANOVA; $p<0.05$) on the length of the P_{11}-12 fibrils. The analysis also revealed that, Na^+ ion concentration in the salt solution, GAG molar ratio and the combination of the two had a significant effect (2-way ANOVA; $p<0.05$) on the widths of the P_{11}-12 fibrils. The data shown in Figure 6 indicates that the longest fibrils formed by the P_{11}-12 peptide were at a GAG molar ratio of 1:16 in both 130 mM and 230 mM Na^+ salt solutions.

Figure 5

Figure 6

When considering the overall morphology of the SAPs and SAP-GAG mixtures (Figure 2, 3 and 4), generally those SAP and SAP-GAG mixtures that exhibited higher β-sheet formation tended to exhibit denser networks of fibrils and fibres, with a greater proportion of junction points. The presence of these nanofibrilar networks with interwoven morphology indicated the formation of self-supporting hydrogels. This was not the case for P_{11}-12 at both GAG molar ratios and in both Na^+ salt solutions. SAP P_{11}-12 precipitated out of solution and formed solid white floculates, some of which were observed in the TEM images (Figure 4, images B & E). These clumps appeared to interact with each other to form bundles and small networks as was the case in the other gels. The low percentage of β-sheet formation exhibited in the FTIR analysis could be linked to the irregular fibril morphology and this may be due to the unexpected formation of nanotubes although these were not widely observed.
It is important to note that variations and trends identified in the widths and lengths of the SAPs and SAP-GAG mixtures may not be directly related to the GAG molar ratio and concentration of the Na^+ salt solution. Peptide and peptide-GAG samples were left to dry before TEM analysis and therefore it is possible that the drying process could have had an effect on the fibril/fibre formation and/or association of the structures.
Nevertheless, images show that P_{11}-4 and P_{11}-8 alone and with GAG demonstrated a characteristic network of entangled fibres/fibrils, an indicator that the SAPs have undergone hierarchical self-assembly to form these structures. Despite having some of the longest and thickest fibrils, P_{11}-12, did not demonstrate this characteristic network. Considering the morphological data and coupling this with the FTIR P_{11}-12 would not be considered a good candidate for future biological studies. It would appear that the GAGs have a negative effect on the self-assembling and morphological properties of P_{11}-12, which is not desirable for the intended application.

Rheology

Rheology has previously been used to explore the biomechanical properties of various peptide hydrogels and also, to study their gelation mechanisms during and after flow. [6] The peptides were firstly subjected to an amplitude sweep in a shear strain

controlled mode from 0.01-100% at 1Hz and 20Hz (with a 10 minute pause inbetween to allow for recovery). A strain value that lay within the linear viscoelastic region (LVER) was chosen. Frequency sweeps were then run to determine the dynamic modulus of the hydrogel samples. The sweeps were run between 1 and 20 Hz at the pre-determined strain that was established from the amplitude sweep. Peptide hydrogels were allowed to equilibrate for 15 minutes once loaded, prior to the start of testing. All tests were performed in replicates of three and at 37^0C (Figure 7).

For the peptides alone, the shear moduli of P_{11}-4 and P_{11}-8 were higher than those of P_{11}-12 by two orders of magnitude. This indicates that there was significant variation between the glutamine based peptide gels (P_{11}-4 and P_{11}-8) and the serine based peptide gels (P_{11}-12) in both Na^+ salt solutions throughout the frequency range (Figure 7). Increasing the Na^+ salt concentration increased the moduli of P_{11}-12, indicating that the positively charged serine based peptide was interacting positively with the increased concentration of Na^+ ions in the higher ionic strength solution. This increased its mechanical stiffness 3 fold (Figure 7C & F). This was concurrent with the FTIR analysis, as its β-sheet component also increased. A very slight increase in the shear moduli was observed in the 130mM Na^+ salt solution for peptides P_{11}-4 and P_{11}-8. This effect was not as apparent in the P_{11}-12 samples in either of the Na^+ salt solutions, suggesting that as the frequency is increasing the P_{11}-4 and P_{11}-8 samples are getting stiffer.

The addition of a higher amount of GAG (1:16) to P_{11}-4, caused a significant variation in the shear modulus of P_{11}-4 in the 130 mM Na^+ salt solution but this was not the case in the 230 mM Na^+ salt solution (Figure 7A & D). In the 230 mM Na^+ salt solution and increasing the GAG molar ratio showed no significant variation in the stiffness of the gel produced. However, an increase in the shear moduli was also observed across the frequencies studied. This was very noticeable in the 130mM Na^+ salt solution. Nevertheless, the data indicated that the gels of P_{11}-4 in the 230 mM Na^+ salt solution at both GAG molar ratios were stiffer than those prepared in the 130 mM Na^+ salt solution.

Similarly with the P_{11}-8 gels in the 130 mM Na^+ salt solution, there was no significant variation in the mechanical stiffness of the control gels (peptide alone) compared to the gels with a small amount of GAG (1:64). Significant variation in the shear moduli ($p<0.05$) was observed when a larger amount of GAG (1:16) was added; when compared to both the control and the 1:64 GAG molar ratio. In this case increasing the amount of GAG reduced the stiffness of the gels (Figure 7B & E).

Conversely, with P_{11}-8 in the 230 mM Na^+ salt solution, there was significant variation observed in the mechanical stiffness's when the control gels were compared to the gels with both molar ratios of GAG, across all frequencies. In this particular Na^+ salt solution the addition of more GAGs, decreased the shear moduli and reduced the gel stiffness. Comparing the effects that the Na^+ salt solution had on the shear moduli and mechanical properties of the gels revealed that, there was significant variation between the P_{11}-8 control samples. An increase in the ionic strength of the Na^+ salt solution (230 mM) increased the mechanical stiffness of the gel. The data indicated that the gels formed at 230 mM with no GAG (control sample) had the highest mechanical stiffness.

P_{11}-12 samples exhibited solid-like behaviour (Figure7C & F) as the samples tested were biphasic (i.e. fluid and flocculated peptide). As the GAG molar ratio was increased in the 130 mM Na^+ salt solution, an increase in the mechanical stiffness of the P_{11}-12 gels was observed, across all frequencies. Conversely, for P_{11}-12 in the 230 mM Na^+ salt solution a different effect on the mechanical stiffness was observed. The

addition of a small amount of GAG (1:64) decreased the shear moduli but a further increase in the amount of GAG added caused the opposite effect, across all frequencies (Figure 7C & F). The gels produced at the higher GAG molar ratio (1:16) were less stiff than the P_{11}-12 control sample.

The P_{11}-12-GAG gels behaved very differently to P_{11}-4 and P_{11}-8, which was observed solely from comparing Figure 7C & F to Figure 7A, B, D & E. There was significant variation in the mechanical stiffness's between both P_{11}-12 control gels and between the gels at higher GAG molar ratio in both Na^+ salt solutions (across all frequencies). The control gel in the 230 mM Na^+ salt solution was stiffer than all the gels studied for P_{11}-12.

Given the two salt solutions that these peptides were tested under, it was clear that the addition of the GAG allows for the mechanical properties of the peptide hydrogels to be tuned over a range of up to four orders of magnitude. In all peptide samples tested the, elastic component was found to be greater than the viscous component, demonstrating solid-like behaviour of these hydrogels and in some cases, even exhibiting shear thinning characteristics, that may be advantageous for their future uses in cartilage regeneration.

Experimental

Materials

Peptides, P_{11}-4, P_{11}-8 and P_{11}-12 were purchased from CS-BIO, and had percentage purities of 95%, 77.6% and 79.7% respectively. The peptides were evaluated at 10 $mg.ml^{-1}$ in all experiments. The amount of each peptide supplied that was weighed to achieve the desired concentration was calculated based upon the peptide purity.

The GAG selected for evaluation was chondroitin sulphate sodium salt (C4484 Sigma, CAS No. 9007-28-7). Two molar ratios of GAG: peptide of 1:64 and 1:16 were assessed. In order to calculate the weight of peptide to obtain the correct molarity, the average molecular weight of the chondroitin sulphate (54,000 Da) was taken into consideration.

Preparation of Na^+ salt solutions

The peptides, GAG and peptide/GAG mixtures were studied in two aqueous salt solutions containing varying Na^+ ion concentrations (130 mM and 230 mM). The two salt solutions were prepared as described by Urban (1994) representing the highest and lowest ion concentrations present in articular cartilage.[23] For the Fourier transform infrared spectroscopy analyses the salts were dissolved in deuterated water (D_2O). For all other analyses the salts were dissolved in distilled water.

Preparation of peptide controls: P_{11}-4, P_{11}-8, and P11-12

Dry lyophilised peptides were weighed and 3.5 ml of the 130 mM or 230 mM Na^+ salt solution was added, samples were immediately sonicated for 10 min. Peptides were then monomerised by adjusting the pH or [pD] (above pH 12 [11.6] for P_{11}-4 and below pH 3 [2.6] for P_{11}-8 and P_{11}-12) using 10-50 µl of 0.1–3 M HCl or NaOH. Measured pD values quoted here were those following a 0.4 correction value subtracted to the pH meter reading for those samples in deutrated solutions (FTIR samples).[32] The monomeric state was determined by observing the fluidity of the gels (monomeric peptides were clear and exhibited water like properties).

The peptide solutions were then carefully adjusted to pH 7.4 using varying molar aliquots of HCl and NaOH (0.1–3 M). Peptide solutions were then placed in a water bath at 37°C for two hours and stored at 4°C overnight to allow them to equilibrate and

prevent any contamination. The pH was re-measured and re-adjusted to pH 7.4 the following day, making sure to make the final solution up to 4 ml before testing.

Preparation of peptide: chondroitin sulphate (GAG) mixtures:
Mixtures of P_{11}-4, P_{11}-8, and P_{11}-12 with chondroitin sulphate at molar ratios of 1:16 and 1:64 (GAG: peptide) were prepared in the two Na^+ salt solutions. Peptides were weighed, rehydrated in 3 ml of Na^+ salt solution and monomerised as described above. For each desired peptide/ GAG mixture, the corresponding weight of chondroitin sulphate was hydrated in 950 µl of Na^+ salt solution. This GAG suspension was vortexed for approx. 40 secs and sonicated for 5 min at 37ºC. The GAG suspension was added to the monomerised peptide and vortexed for a further 40 secs. The pH was adjusted to 7.4 and the mixture incubated at 37ºC for two hours. Samples were refrigerated overnight (4°C) to allow them to equilibrate and the pH was re-measured and re-adjusted to pH 7.4 the following day, making sure to make the final solution up to 4 ml before testing.

Preparation of GAG control
Pre-weighed chondroitin sulphate was hydrated in 3.95 ml of Na+ salt solution. Samples were vortexed for approx. 40 secs and sonicated for 10 min at 37ºC. The pH was then adjusted to 7.4 using the remaining 50 µl volume of HCl and NaOH aliquots to make the total volume up to 4 ml.

Methods

1. Fourier Transform Infrared Spectroscopy.
Secondary structures of the peptides were determined using FTIR on a Thermo Nicolet 6700 spectrometer, controlled with OMINC 7.3 SP1 software. Aliquots of approx. 40 µl of the samples prepared in D_2O, were placed into Thermo HT-32 demountable cells between two CaF_2 windows and a 0.025 mm copper spacer. Each spectrum was an average of 32 scans taken at a resolution of 4 cm^{-1} at room temperature, one replicate per sample was analysed. A background spectrum of the two D_2O Na^+ salt solutions was taken prior to any sample analysis and subtracted from all sample spectra. The relative content of β-sheet was calculated by fitting the experimental spectra peaks to the second derivative of the amide I' region (1720-1580 cm^{-1}) and assigning the peaks as stated in the literature.[33, 34] The relative amount of β-sheet structure present was then estimated by calculating the percentage area corresponding to the β-sheet band.[35]

2. Transmission Electron Microscopy (TEM).
Carbon-coated copper grids (400 mesh grids, Agar scientific) were placed coated side down on the surface of a 10 µl droplet of the sample to be analysed, for 1 min and then blotted on filter paper to remove excess. Grids were then placed on a 10 µl droplet of 2% (20 $mg.ml^{-1}$) of uranyl acetate for 30 secs for negative staining and then blotted against double folded Whatman 50 filter paper and left to dry. Images were recorded on a JEM-1400 Joel Microscope equipped with an AMT ERB bottom mounted digital CCD camera. Only one replicate per sample was analysed. ImageJ was used to trace over the fibrils to determine the lengths and widths of 20 individual fibres/fibrils for each peptide and peptide-GAG mixtures in order to get an average length and width for the SAP fibrils.

3. Rheology.
All rheological measurements were carried out on a Malvern Kinexus rheometer. rSpace Kinexus by Malvern Instruments was used to control the rheometer and export

raw data. A coned-plate geometry (50 mm diameter, gap of 0.0330 mm) was used with a cone angle of 1º. All tests were run at 37ºC, using a solvent trap (SU0005 PLC). Three replicate samples were measured in triplicate for each SAP-GAG mixture in the two Na^+ salt solutions. Each sample had a total volume of 4 ml. For each replicate 1 ml was applied to the rheometer. Samples were firstly subjected to an amplitude sweep. Two amplitude sweeps were performed in a shear strain controlled mode from 0.01-100%, one at 1 Hz and another at 20 Hz with a 10 minute pause in-between the two to allow the peptides to equilibrate. A strain value that lay within the linear viscoelastic region (LVER) was chosen. Frequency sweeps were then run to determine the dynamic modulus of the hydrogel samples. The sweeps were run between 1 and 20 Hz at the pre-determined strain that was established from the amplitude sweep. Peptide hydrogels were allowed to equilibrate for 15 minutes once loaded, prior to the start of testing.

Data analysis

For the rheology study, the null hypothesis that was tested was that all three independent variables (peptide, molar ratio and Na^+ salt concentration) would have no significant effect on the dependant variable (shear modulus, stiffness) at 1Hz. A three way analysis of variance (ANOVA) was performed on the rheological data acquired using SPPS (Version 20). This was carried out using the univariate analysis of variance tool and selecting the full factorial analysis, which not only showed the significance of the individual independent variables but also showed the 2 way and 3 way interactions between the independent variables and their significances on the dependant variable.

In the TEM study, the null hypothesis that was tested was that neither the GAG molar ratio nor concentration of Na^+ ions would have any effect on the lengths and widths of the peptide fibrils. Two-way ANOVA was used to analyse the data using SPSS. Similarly, the univariate analysis of variance tool was used with full factorial analysis, which showed the significant effects of the individual independent variables on the dependant variable.

Conclusions

The mechanical properties of the SAP-GAG mixtures were influenced by the ionic interactions between the negatively charged GAGs and the positively/negatively charged peptides as well as their interaction with the surrounding ionic Na^+ salt solution. This study showed that the addition of another charged bio-polymer and the change in the ionic strength of the surrounding solution had a large effect on the stiffness of the individual peptide hydrogels by either promoting a greater number of entanglements in particular peptides or by inhibiting the peptides ability to form entanglements and junction points.

The addition of the GAG not only provided the high charge found in native tissue, which contributes to the hydration and function of cartilage, but at an optimum molar ratio it improved the rheological properties of some of the resulting gels. Increasing the Na^+ ion concentration (as found in the surface of cartilage) allowed for the investigation of how the peptides would behave in in vivo conditions and also the effect that this had on the rheological properties of the resulting gels.

Analysis of the rheology data by three-way analysis of variance revealed the combined effect of the three variables (peptide, GAG molar ratio and Na+ salt concentration) and their effect on the overall shear modulus at 1Hz. It was clear from the statistical analysis that all variables had a significant effect on the shear modulus ($p<0.05$). However, the combined effect of the choice of peptide and the Na+ ion

concentration in the salt solution did not have a significant effect on the overall shear modulus ($p>0.05$).

Overall, the presence of GAG decreased the gel stiffness of the glutamine based peptides (P_{11}-4 and P_{11}-8) at high GAG concentration but slightly increased the stiffness at low GAG concentrations; however the corresponding peptides alone were mechanically stiffer. By contrast, for the serine based peptide (P_{11}-12) gel stiffness was increased at high GAG concentrations, but the stiffness values were still much lower than the glutamine based peptides.

New SAP-GAG hybrid materials have been developed with adjustable mechanical properties. Their ability to self-assemble and the incorporation of chondroitin sulphate, at the correct molar ratio makes them feasible candidates for a minimally invasive therapy to aid in the restoration of mechanical properties to early stage osteoarthritic cartilage. FTIR and TEM studies have highlighted the SAP-GAG combinations that were able to form characteristic self-supporting gels able to produce characteristic entangled fibrilar networks similar to those found in native cartilage. Alongside this, the rheological studies at (1Hz) determined that P_{11}-4 and P_{11}-8 peptide-GAG combinations (Figure 8), were among the stiffest.

The combination of these studies has identified that two of the three SAPs demonstrate all of the three favourable properties: high β-sheet percentage, characteristic entangled fibrilar networks and a high stiffness coefficient.

In conclusion, the data presented in this study indicates that P_{11}-4 and P_{11}-8-chondroitin sulphate mixtures have properties which make them suitable candidates for further investigation for their capacity to restore the biomechanical properties of GAG depleted tissues such as early stage OA cartilage.

Acknowledgements

This work was supported by EPSRC and the Wellcome Trust.
JF is a NIHR Senior investigator. JF and EI are supported in part by the NIHR Leeds Musculoskeletal biomedical Research Unit

Statement of conflict of interests

JF acts as a consultant to DePuySynthes, Invibio, Simulation Solutions and Tissue Regenix
EI acts as a consultant to Tissue Regenix and DePuySynthes

References

1. Lopez AD, Mathers CD, Ezzati M, Jamison DT, Murray CJL. Global and regional burden of disease and risk factors, 2001: systematic analysis of population health data. The Lancet. 2006;367(9524):1747-57.

2. Arthritis Research UK. Osteoarthritis in General Practice: Data and Perspectives. Arthritis Research UK, 2013.

3. Otsuki S, Nakajima M, Lotz M, Kinoshita M. Hyaluronic acid and chondroitin sulfate content of osteoarthritic human knee cartilage: Site-specific correlation with weight-bearing force based on femorotibial angle measurement. Journal of Orthopaedic Research. 2008;26(9):1194-8.

4. Mankin HJ, Lippiello L. The glycosaminoglycans of normal and arthritic cartilage. Journal of Clinical Investigation. 1971;50(8):1712.

5. Katta J, Stapleton T, Ingham E, Jin Z, Fisher J. The effect of glycosaminoglycan depletion on the friction and deformation of articular cartilage. Proceedings of the Institution of Mechanical Engineers, Part H: Journal of Engineering in Medicine. 2008;222(1):1-11.

6. Aggeli A, Bell M, Boden N, N. Keen J, C. B. McLeish T, Nyrkova I, et al. Engineering of peptide [small beta]-sheet nanotapes. Journal of Materials Chemistry. 1997;7(7):1135-45.

7. Zhang S, Gelain F, Zhao X. Designer self-assembling peptide nanofiber scaffolds for 3D tissue cell cultures. Seminars in Cancer Biology. 2005;15(5):413-20.

8. Bell CJ, Carrick LM, Katta J, Jin Z, Ingham E, Aggeli A, et al. Self-assembling peptides as injectable lubricants for osteoarthritis. Journal of Biomedical Materials Research Part A. 2006;78A(2):236-46.

9. Firth A, Aggeli A, Burke JL, Yang X, Kirkham J. Biomimetic self-assembling peptides as injectable scaffolds for hard tissue engineering. Nanomedicine. 2006;1(2):189-99.

10. Kirkham J, Firth A, Vernals D, Boden N, Robinson C, Shore R, et al. Self-assembling peptide scaffolds promote enamel remineralization. Journal of dental research. 2007;86(5):426-30.

11. Kerstin MG, Adriana C, Virany Y, He D, Songtao S, Gottfried S, et al. Self-Assembling Peptide Amphiphile Nanofibers as a Scaffold for Dental Stem Cells. Tissue Engineering Part A. 2008;14(12):2051-8.

12. Schneider A, Garlick JA, Egles C. Self-assembling peptide nanofiber scaffolds accelerate wound healing. PLoS One. 2008;3(1):e1410.

13. Kyle S, Aggeli A, Ingham E, McPherson MJ. Production of self-assembling biomaterials for tissue engineering. Trends in biotechnology. 2009;27(7):423-33.

14. Kyle S, Aggeli A, Ingham E, McPherson MJ. Recombinant self-assembling peptides as biomaterials for tissue engineering. Biomaterials. 2010;31(36):9395-405.

15. Shah RN, Shah NA, Lim MMDR, Hsieh C, Nuber G, Stupp SI. Supramolecular design of self-assembling nanofibers for cartilage regeneration. Proceedings of the National Academy of Sciences. 2010;107(8):3293-8.

16. Brunton PA, Davies RPW, Burke JL, Smith A, Aggeli A, Brookes SJ, et al. Treatment of early caries lesions using biomimetic self-assembling peptides - a clinical safety trial. Br Dent J. 2013;215(4):E6-E.

17. Maude S, Ingham E, Aggeli A. Biomimetic self-assembling peptides as scaffolds for soft tissue engineering. Nanomedicine. 2013;8(5):823-47.

18. Boekhoven J, Stupp SI. 25th Anniversary Article: Supramolecular Materials for Regenerative Medicine. Advanced Materials. 2014;26(11):1642-59.

19. Rubert Pérez CM, Stephanopoulos N, Sur S, Lee S, Newcomb C, Stupp S. The Powerful Functions of Peptide-Based Bioactive Matrices for Regenerative Medicine. Ann Biomed Eng. 2015;43(3):501-14.

20. Aggeli A, Nyrkova IA, Bell M, Harding R, Carrick L, McLeish TCB, et al. Hierarchical self-assembly of chiral rod-like molecules as a model for peptide β-sheet tapes, ribbons, fibrils, and fibers. Proceedings of the National Academy of Sciences. 2001;98(21):11857-62.

21. Maude S, Miles DE, Felton SH, Ingram J, Carrick LM, Wilcox RK, et al. De novo designed positively charged tape-forming peptides: self-assembly and gelation in physiological solutions and their evaluation as 3D matrices for cell growth. Soft Matter. 2011;7(18):8085-99.

22. Miles DE, Mitchell EA, Kapur N, Beales PA, Wilcox RK. Peptide:glycosaminoglycan hybrid hydrogels as an injectable intervention for spinal disc degeneration. Journal of Materials Chemistry B. 2016;4(19):3225-31.

23. Urban J. The chondrocyte: a cell under pressure. Rheumatology. 1994;33(10):901-8.

24. Danion F, Varraine E, Bonnard M, Pailhous J. Stride variability in human gait: the effect of stride frequency and stride length. Gait & Posture. 2003;18(1):69-77.

25. Mason SJ, Legge GE, Kallie CS. Variability in the length and frequency of steps of sighted and visually impaired walkers. Journal of visual impairment & blindness. 2005;99(12):741.

26. Arrondo JLR, Muga A, Castresana J, Goñi FM. Quantitative studies of the structure of proteins in solution by fourier-transform infrared spectroscopy. Progress in Biophysics and Molecular Biology. 1993;59(1):23-56.

27. Barth A. Infrared spectroscopy of proteins. Biochimica et Biophysica Acta (BBA) - Bioenergetics. 2007;1767(9):1073-101.

28. Kong J, Yu S. Fourier Transform Infrared Spectroscopic Analysis of Protein Secondary Structures. Acta Biochimica et Biophysica Sinica. 2007;39(8):549-59.

29. Elfrink K, Ollesch J, Stöhr J, Willbold D, Riesner D, Gerwert K. Structural changes of membrane-anchored native PrPC. Proceedings of the National Academy of Sciences. 2008;105(31):10815-9.

30. Lamm MS, Rajagopal K, Schneider JP, Pochan DJ. Laminated morphology of nontwisting β-sheet fibrils constructed via peptide self-assembly. Journal of the American Chemical Society. 2005;127(47):16692-700.

31. Kubelka J, Keiderling TA. Differentiation of β-Sheet-Forming Structures: Ab Initio-Based Simulations of IR Absorption and Vibrational CD for Model Peptide and Protein β-Sheets. Journal of the American Chemical Society. 2001;123(48):12048-58.

32. Glasoe PK, Long FA. USE OF GLASS ELECTRODES TO MEASURE ACIDITIES IN DEUTERIUM OXIDE1,2. The Journal of Physical Chemistry. 1960;64(1):188-90.

33. Bradley M. Curve fitting in Raman and IR spectroscopy: basic theory of line shapes and applications. Thermo Fisher Scientific, Madison, USA, Application Note. 2007;50733.

34. Stuart BH. Biological applications. Infrared spectroscopy: fundamentals and applications. 2004:137-65.

35. Stuart BH, George B, McIntyre P. Modern Infrared Spectroscopy: Wiley; 1996.

Peptide	Amino Acid Sequence	Net charge at pH 7.4
P_{11}-4	$CH_3COQQRFEWEFEQQNH_2$	-2
P_{11}-8	$CH_3COQQRFOWOFEQQNH_2$	+2
P_{11}-12	$CH_3COSSRFOWOFESSNH_2$	+2
Q=Glutamine, R=Arginine, F=Phenylalanine, E=Glutamic acid, W=Tryptophan, O=Ornithine, S=Serine		

Table 1: Peptide primary structures, and their net charges at pH 7.4. Positively charged residues are coloured blue, negatively charged residues are red.

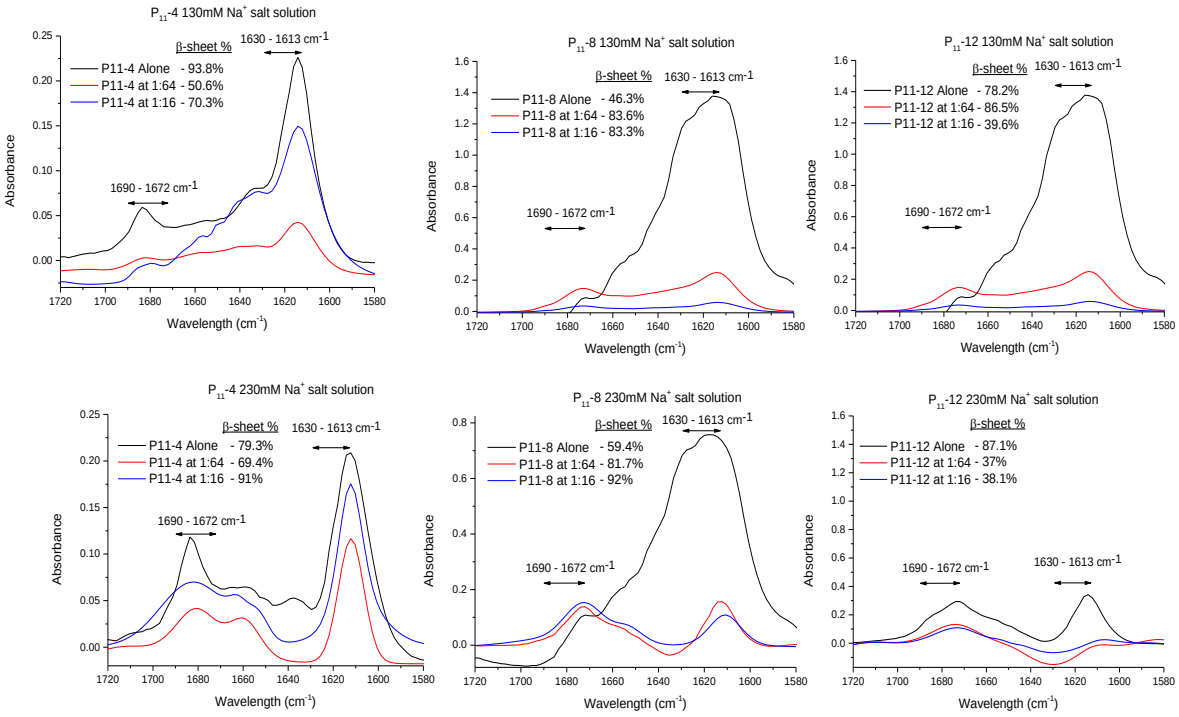

Figure 1: Fitted IR amide I' band of P_{11}-4, P_{11}-8 & P_{11}-12 at 10 mg.ml^{-1} in presence of 130 mM (A) and 230 mM (B) Na+ salt solution at varying GAG molar ratios. The β-sheet percentage was calculated by adding the total area of the peaks showing β-sheet and then dividing them by the areas of all the individual peaks combined for each graph and multiplying by 100. The β-sheet regions are defined by the peaks in the wavelength region of 1630-1613 cm^{-1} and 1690-1672 cm^{-1}.[28]

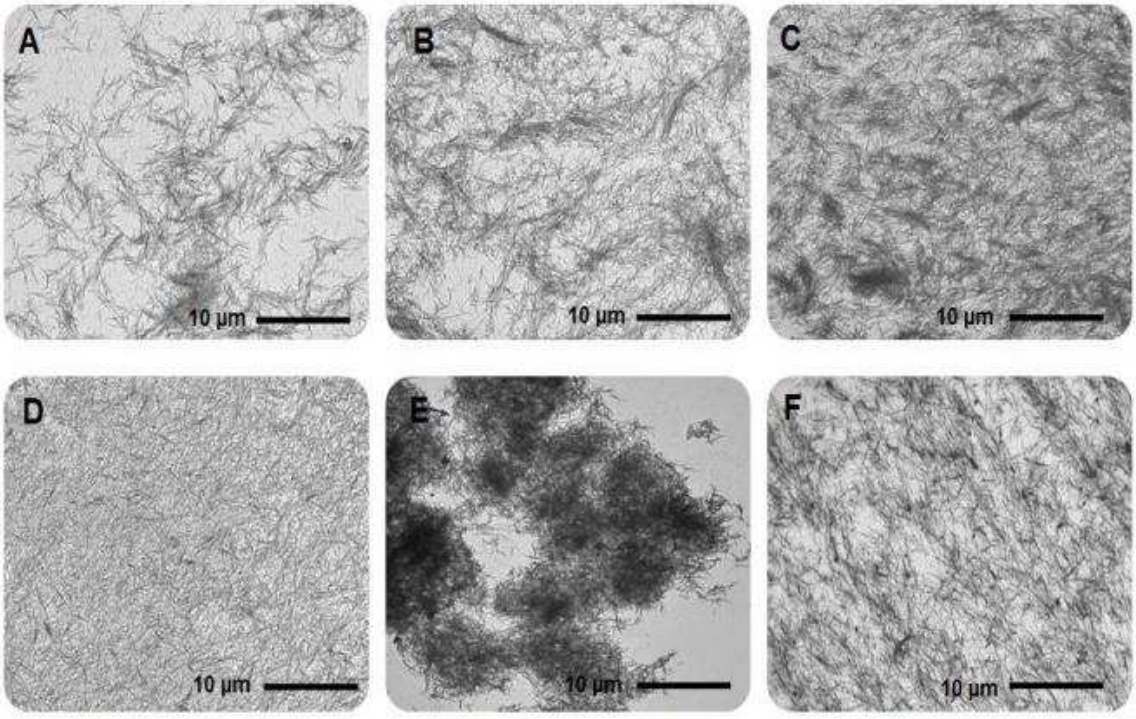

Figure 2: Morphology of the P_{11}-4 peptide in the presence of two Na^+ salt solutions at varying GAG molar ratios (1:16 and 1:64) by TEM. (A) P_{11}-4 in a 230mM Na^+ salt solution, (B) P_{11}-4 at 1:64 GAG molar ratio in a 230mM Na^+ salt solution, (C) P_{11}-4 at 1:16 GAG molar ratio in a 230mM Na^+ salt solution, (D) P_{11}-4 in a 130mM Na^+ salt solution, (E) P_{11}-4 at 1:64 GAG molar ratio in a 130mM Na^+ salt solution, (F) P_{11}-4 at 1:16 GAG molar ratio in a 130mM Na^+ salt solution. Magnification of 500. Individual scale bars (10 µm) are shown for each image.

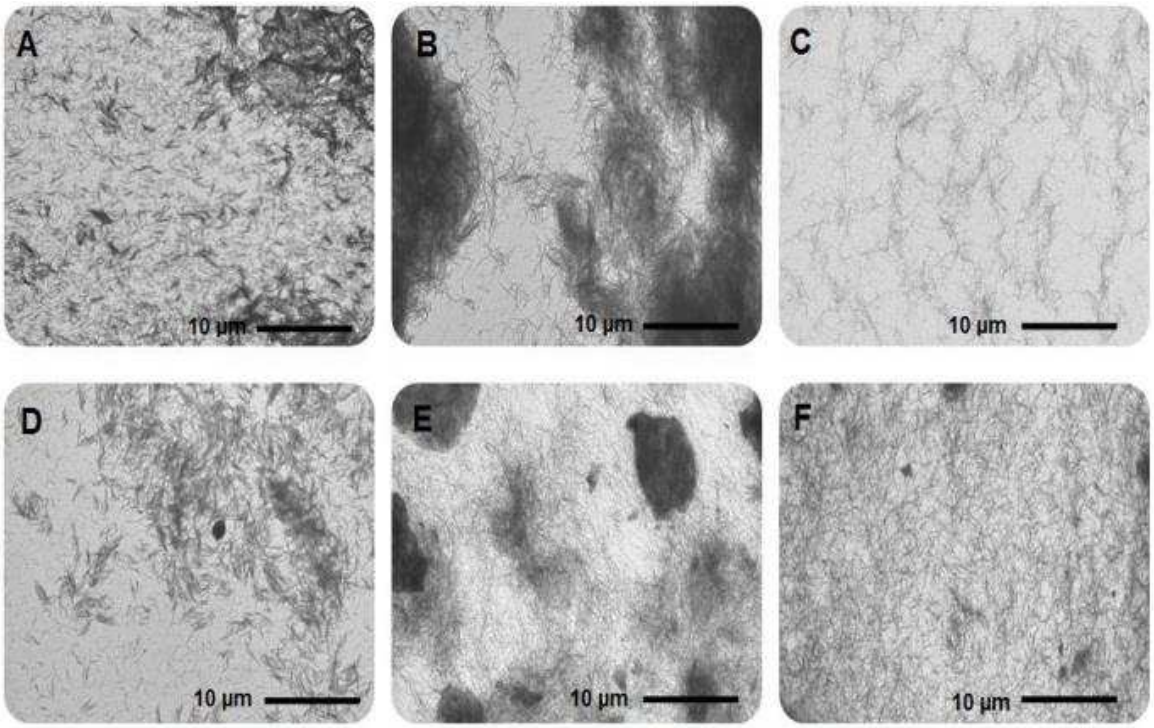

Figure 3: Morphology of the P_{11}-8 peptide in the presence of two Na^+ salt solutions at varying GAG molar ratios (1:16 and 1:64) by TEM. (A) P_{11}-8 in a 230mM Na^+ salt solution, (B) P_{11}-8 at 1:64 GAG molar ratio in a 230mM Na^+ salt solution, (C) P_{11}-8 at 1:16 GAG molar ratio in a 230mM Na^+ salt solution, (D) P_{11}-8 in a 130mM Na^+ salt solution, (E) P_{11}-8 at 1:64 GAG molar ratio in a 130mM Na^+ salt solution, (F) P_{11}-8 at 1:16 GAG molar ratio in a 130mM Na^+ salt solution. Magnification of 500. Individual scale bars (10 µm) are shown for each image.

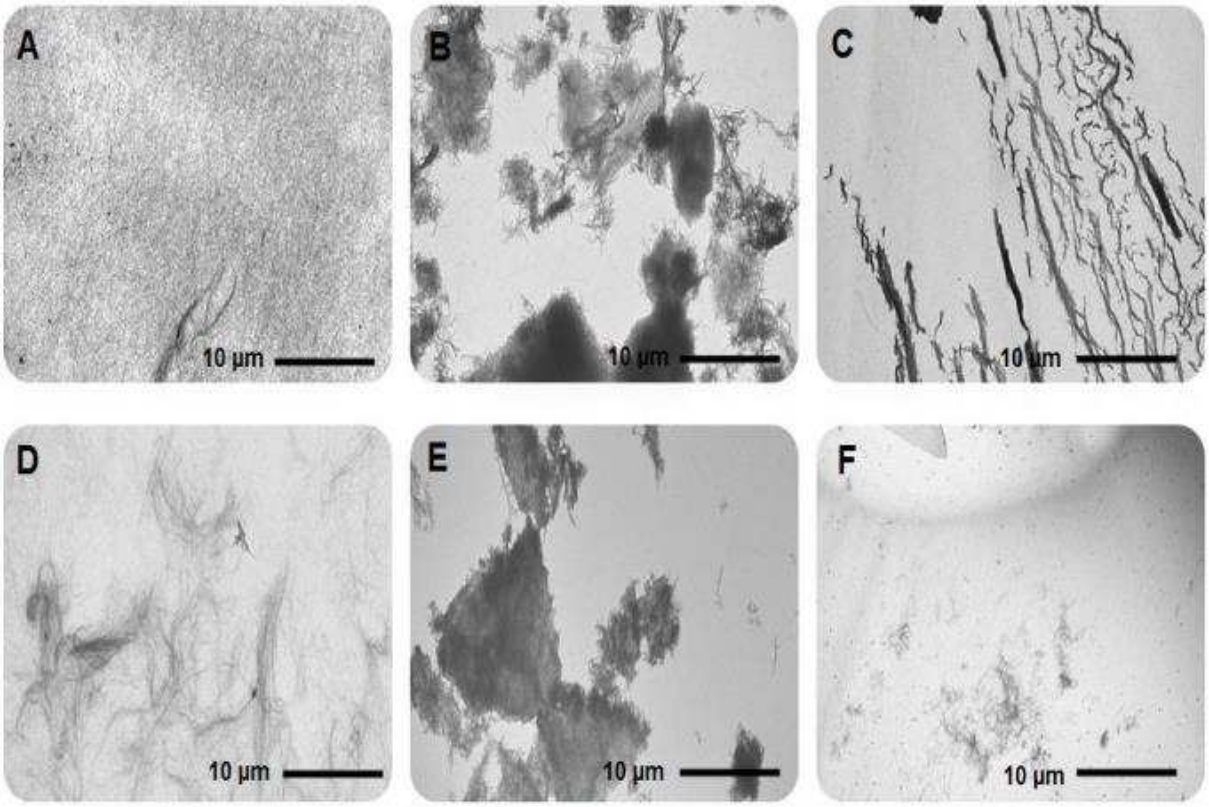

Figure 4: Morphology of the P11-12 peptide in the presence of two Na+ salt solutions at varying GAG molar ratios (1:16 and 1:64) by TEM. (A) P_{11}-12 in a 230mM Na^+ salt solution, (B) P_{11}-12 at 1:64 GAG molar ratio in a 230mM Na^+ salt solution, (C) P_{11}-12 at 1:16 GAG molar ratio in a 230mM Na^+ salt solution, (D) P_{11}-12 in a 130mM Na^+ salt solution, (E) P_{11}-12 at 1:64 GAG molar ratio in a 130mM Na^+ salt solution, (F) P_{11}-12 at 1:16 GAG molar ratio in a 130mM Na^+ salt solution. Magnification of 500. Individual scale bars (10 µm) are shown for each image.

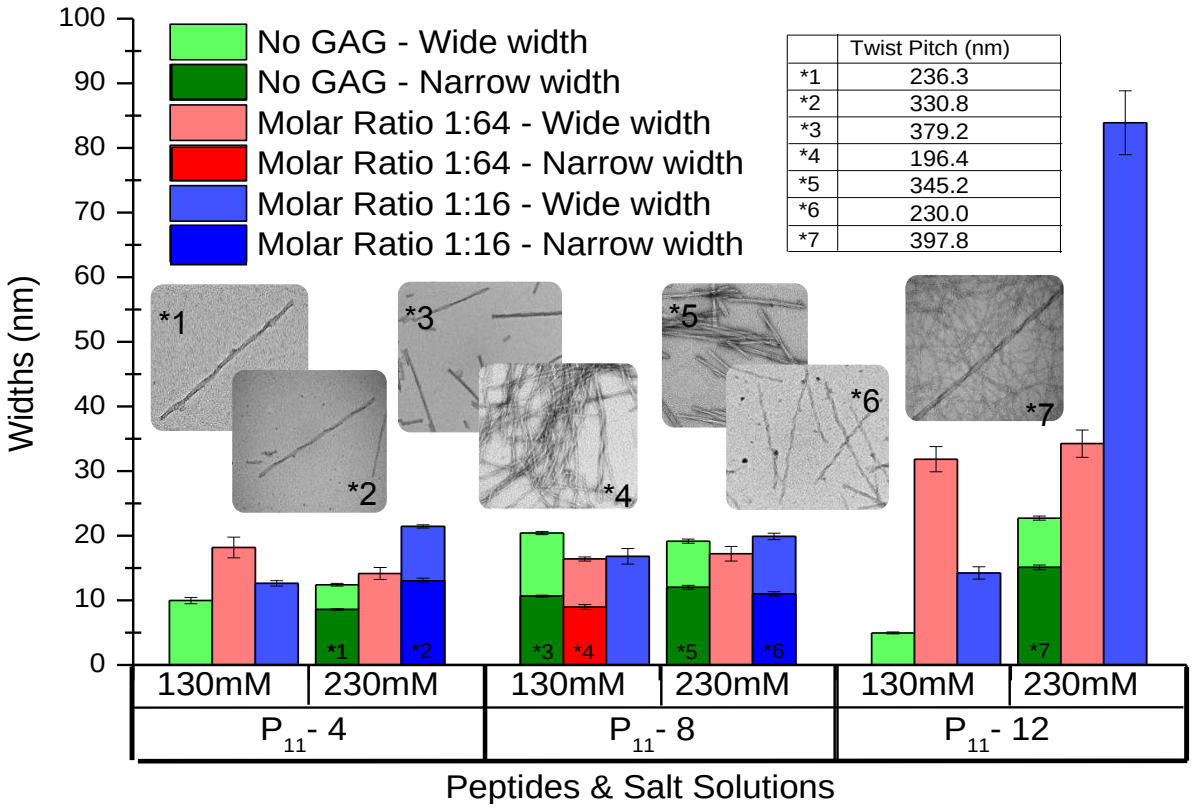

Figure 5: Widths of fibrils of all peptides in two different Na^+ salt solutions at pH 7.4 at varying molar ratios of GAG. Widths of the fibrils were determined from TEM images at a magnification of 30,000 using the software imageJ. 20 fibrils were measured for each sample. The data is presented as the mean (n=20) ± 95% confidence intervals. Data was analysed using two-way analysis of variance and statistical significance was determined at $p<0.05$. This showed that the Na^+ ion concentration in the salt solution, GAG molar ratio and their combined effects had a significant effect on the overall widths of the fibrils formed by all three peptides ($p<0.05$).

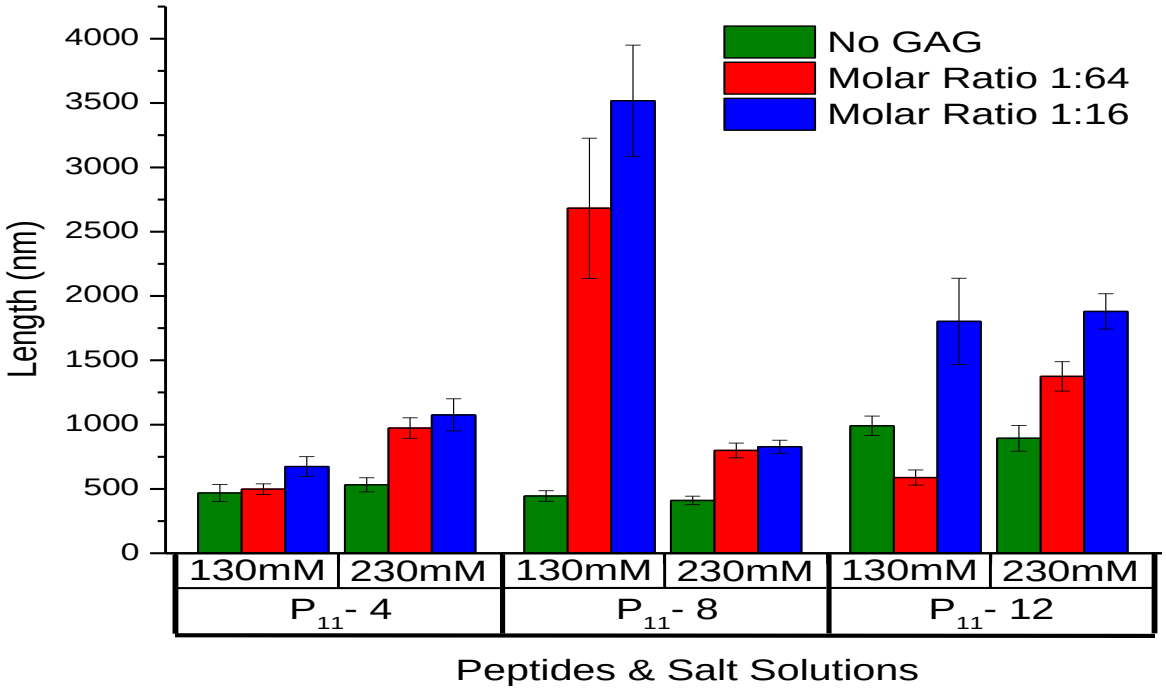

Figure 6: Lengths of fibrils of all peptides in two different Na^+ salt solutions at pH 7.4 at varying molar ratios of GAG. Lengths of the fibrils were determined from TEM images at a magnification of 12,000 using the software imageJ. 20 fibrils were measured for each sample. The data is presented as the mean (n=20) ± 95% confidence intervals. Data was analysed using two-way analysis of variance and statistical significance was determined at $p<0.05$. This showed that for P_{11}-4 and P_{11}-8 the Na^+ ion concentration in the salt solution, GAG molar ratio and their combined effects all had a significant effect on the lengths of the fibres formed ($p<0.05$). For P_{11}-12, the Na^+ ion concentration had no significant effect on the lengths of the fibrils formed by P_{11}-12 ($p=0.084$). However the GAG molar ratio had a significant effect on the length of the fibrils formed by P_{11}-12 ($p<0.05$). The combined effect of GAG molar ratio and Na^+ ion concentration in the salt solution had a significant effect on the length of the fibrils formed by P_{11}-12 ($p=0.049$).

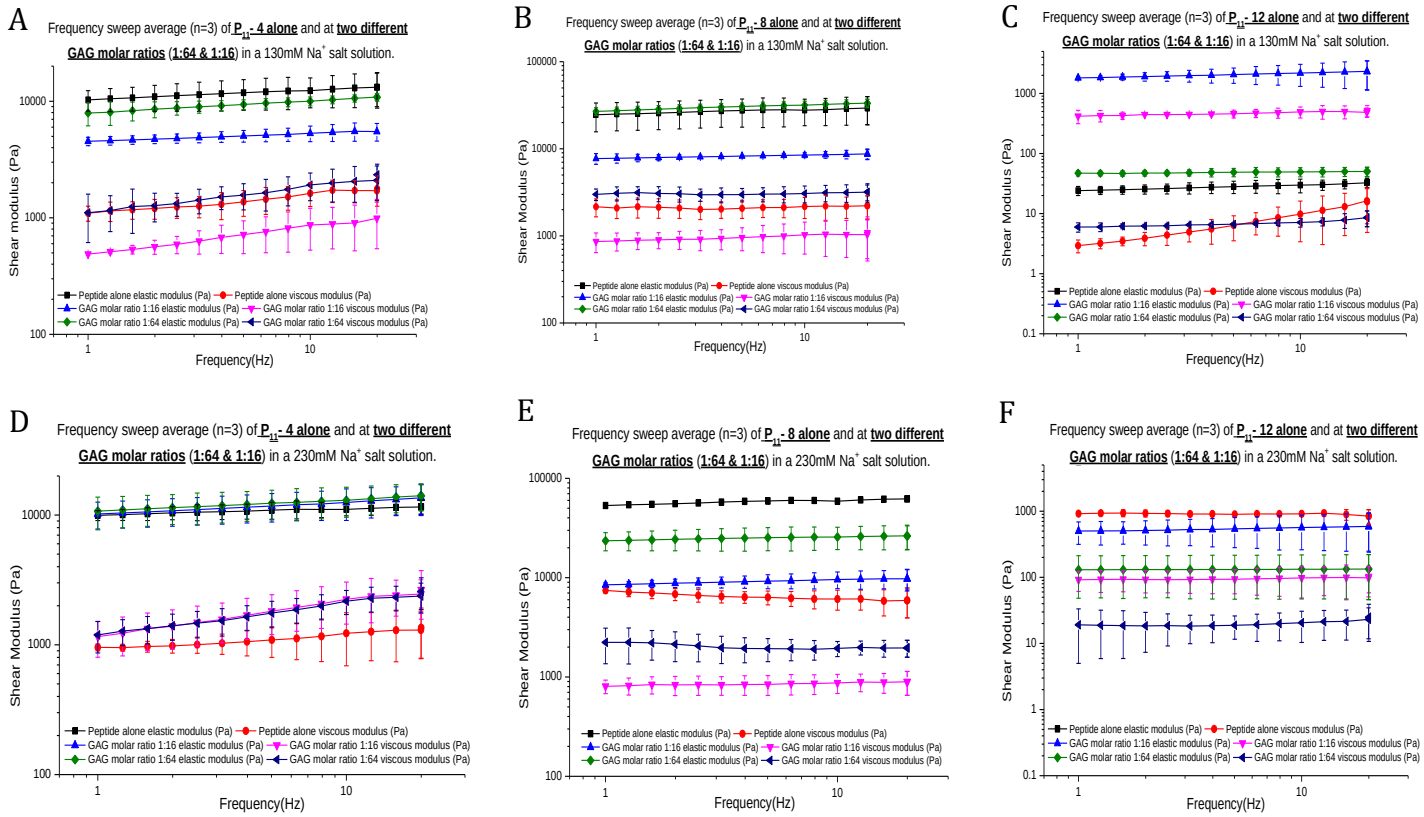

Figure 7: The effect of varying the Na+ ion concentration (130 mM or 230 mM) and GAG molar ratio (1:64 or 1:16) on the mechanical properties of the P_{11}-4, P_{11}-8 and P_{11}-12 gels. Data is presented as the mean (n=3). Individual samples were subject to an amplitude sweep before commencing the test, in order to identify the linear viscoelastic region (LVER). A strain value was then chosen within the middle region of the LVER and the shear moduli (elastic and viscous) were all calculated by running a frequency sweep test between 1Hz & 20Hz.

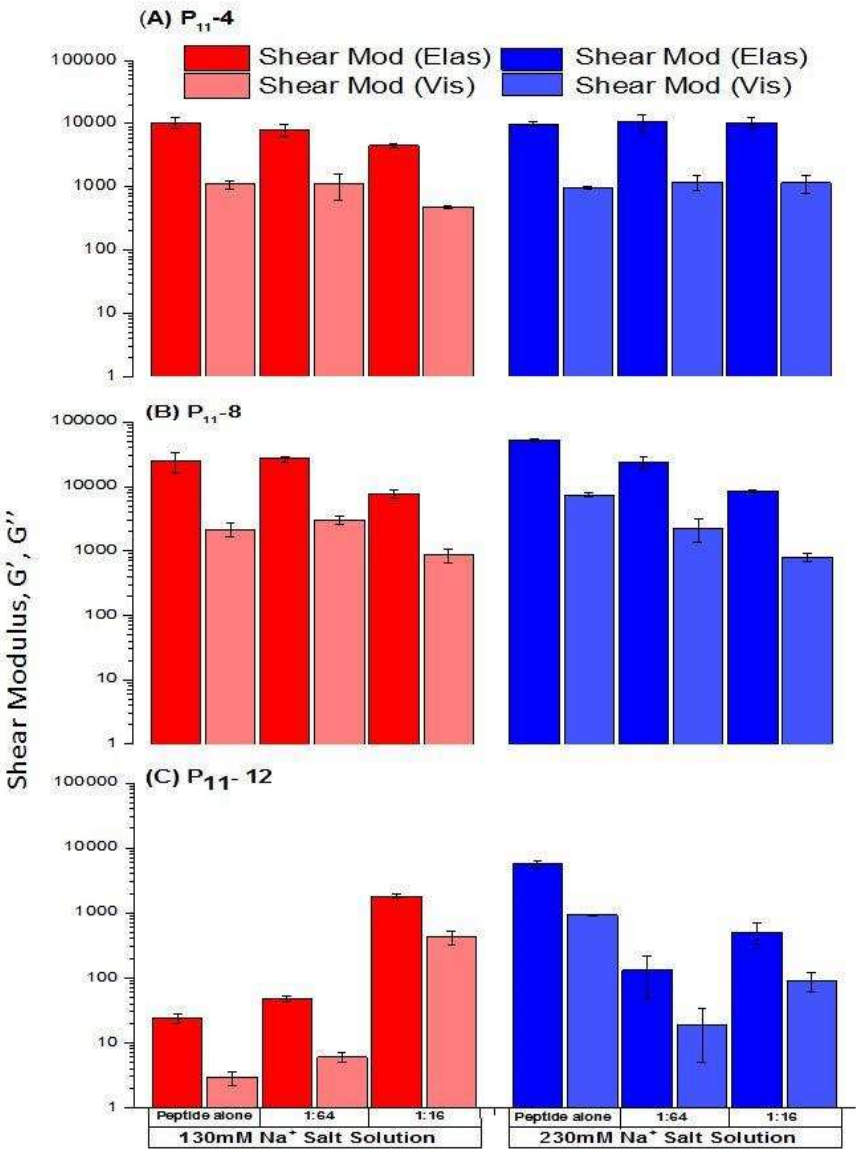

Figure 8: The effect of varying the Na^+ ion concentration (130 mM or 230 mM) and GAG molar ratio (1:64 or 1:16) on the mechanical properties of the P_{11}-4, P_{11}-8 and P_{11}-12 gels. The shear moduli were all taken from the frequency sweep test at 1 Hz. Data is presented as the mean (n=3) ± 95% confidence intervals. Data was analysed using three-way analysis of variance and statistical significance was determined at $p<0.05$. This showed that all the independent variables alone (peptide choice, GAG molar ratio and salt solution) had a significant effect on the mechanical properties across all three peptides ($p=0.00$). Their combined effects showed that peptide choice in combination with the salt solution had no significant effect on the overall mechanical properties of all three peptides ($p=0.065$). For the combined effects of peptide choice, GAG molar ratio and salt solution, there was a significant effect observed in the mechanical properties of all three peptide gels ($p=0.00$).